Density-functional study of the chemisorption of N on and below Fe(110) and Fe(001) surfaces

Štěpán Pick,[1,*] Pierre Légaré,[2] and Claude Demangeat[3]
[1]*J. Heyrovský Institute of Physical Chemistry of the Academy of Sciences of the Czech Republic, v.v.i., Dolejškova 3, CZ-182 23 Prague 8, Czech Republic*
[2]*Laboratoire des Matériaux, Surfaces et Procédés pour la Catalyse, Université Louis Pasteur, 25 rue Becquerel, F-67078 Strasbourg Cedex 2, France*
[3]*Institut de Physique et de Chimie des Matériaux de Strasbourg 23 rue du Loess, F-67034 Strasbourg Cedex 2, France*
(Received 30 January 2007; revised manuscript received 20 April 2007; published 31 May 2007)

We study ordered nitrogen overlayers on and below (110) and (001) surfaces of ferromagnetic bcc iron by using ultrasoft-pseudopotential density-functional calculations. With the exception of (1×1)N/Fe(110), the dissociative surface adsorption of N_2 is predicted to be exothermic, whereas subsurface absorption is always endothermic. The results for chemisorption at Fe(001) agree with experiments; for the (110) face, large deformations induced by N can signalize a tendency to reconstruction. For subsurface nitrogen, some symmetric positions below Fe(001) turn out to be unstable, and large local deformations are present for the stable sites. These structures cannot serve as candidates for nitridized surface films in the initial stage of growth because they are thermodynamically unstable. Below the (110) surface at concentration 0.25 of N, we find even no appropriate metastable sites for nitrogen at zero temperature. The magnetization is markedly suppressed at iron atoms close to N, the controlling parameter being the Fe-N distance and, in some cases, also the induced change of the Fe-Fe separation. In almost all cases we find a small negative magnetic moment on nitrogen atoms.

DOI: 10.1103/PhysRevB.75.195446 PACS number(s): 68.43.Fg, 71.15.Mb, 75.70.−i, 81.65.Lp

I. INTRODUCTION

Catalytic properties of iron surfaces are employed in the industrially important ammonia synthesis. The underlying physics and chemistry have been discussed by a number of authors;[1,2] there is an agreement that N_2 dissociation at surface is the rate-limiting reaction. Together with the entropic barrier, there is an energy barrier (activation energy) of a few tenths of eV per molecule for the dissociation on Fe(001) and Fe(110) surfaces at low nitrogen coverage θ. The barrier height grows with nitrogen coverage.[3] Although the open Fe(111) face offers more favorable conditions for dissociation, it suffers from low stability.[3] (A recent study[4] of N_2 dissociation on tungsten surfaces indicates, moreover, that correct understanding of the kinetics can be rather involved.) Experimental studies of nitrogen on iron surfaces have been performed to elucidate structural and partly also electronic properties.[3,5–9] Recently, also density-functional theory (DFT) results for nitrogen on selected Fe surfaces became available.[2,10] It is useful to mention also thorough computational studies of oxygen[11] and carbon[12] adsorption on Fe, and their penetration below the surface. For nonzero temperature and nitrogen-atmosphere pressure, the equilibrium is controlled by chemical potentials. Hence, energetically unfavorable structures can appear especially if the energy loss is not large. Also metastable forms can, in principle, be prepared. Numerous experiments provide information on adsorbate structures on solid surfaces at vacuum conditions. At high gas pressures, three-dimensional compound films often grow. It is interesting to know whether extremely thin films with gas atoms in subsurface positions might be thermodynamically stable at intermediate conditions that later would facilitate the compound growth.[11] In our case, most of the simple subsurface structures appear to be energetically highly unfavorable or even unstable. The calculation of $p(2\times2)$N subsurface structures provides approximate information on subsurface absorption at low N concentrations. Since the main mechanism seems to be always the formation of Fe-N bonds of apppropriate length, the results should reflect the main features correctly. However, to allow for better optimization of Fe-Fe bonds in highly deformed lattices, larger elementary cell should be used. Hence, our results can somewhat overestimate the endothermicity of the N subsurface dissolution at low concentrations.

Besides catalysis, the behavior of N near the Fe surface is of interest in metallurgy.[13–15] Generally, some N_2 molecules dissociate and penetrate into the metal where they occupy randomly interstitial positions[16] at low concentrations. Nitrogen solubility increases (decreases) with increasing temperature for bcc (fcc) Fe which means that the process is endothermic (exothermic) (Refs. 13, pp. 150–151, and 14, p. 90). This relation follows (at constant pressure) from the van 't Hoff equation[17]

$$d(\ln K_c)/dT = \Delta U/RT^2, \tag{1}$$

where K_c is the equilibrium constant for the reaction expressed in concentrations and, as usual, T is the temperature, U the internal energy, and R the gas constant. The energy loss per nitrogen atom dissolved in bcc iron is[13] about 0.3 eV. In practice, nitride overlayers are grown on iron to improve surface mechanical and anticorrosive properties.[15,18] Several nitrides of iron are known including very complex ones.[18–20] Most often studied is, however, the ferromagnetic compound Fe_4N.[13,19,21–26] This *antiperovskite* crystal can be viewed as fcc iron crystal with nitrogen in the center of the cube. N has thus six Fe nearest neighbors at a distance of 1.895 Å. The magnetization of these Fe atoms is lower (probably $\lesssim 2\mu_B$ despite some difference in values obtained

in Refs. 19, 23, 25, and 26) than in the bcc Fe crystal and also than in fcc iron with a lattice constant of Fe_4N.[19] The value of the moment in Fe_4N is quite sensitive to volume changes.[23,25] Paramagnetic nitrides of iron exist as well.[27] For various magnetic iron nitrides, theory predicts[19] a very small *negative* magnetic moment on N. According to Ref. 28, there is a strong magnetic polarization of electronic states at the Fermi level E_F of Fe_4N which should result in spin-polarized transport effects. The presence of similar phenomena at adsorbate-covered magnetic surfaces might be of interest. Actually, it is known[13] that Fe_4N compounds grow on Fe surfaces at sufficient N_2 gas pressure. In the very early stages, however, three-dimensional germs (nuclei) of Fe_8N (or some similar structures) grow first. The three-dimensional phases can accommodate more gas atoms than the two-dimensional ones. As will be mentioned below, reconstruction takes place on the (110) face as well as at the (001) face of Fe_4N that is closely related to our topic. These facts complicate predictions of the structures at the beginning of nitride(s) growth.

It has been suggested[3,6,7] that there is an analogy between nitridized Fe surfaces and surfaces of Fe_4N. For the (001) surface, the resemblance is rather direct by supposing that Fe_4N crystal is (i) terminated by the (001) plane containing nitrogen atoms and (ii) the latter atoms move vertically towards the vacuum. It is, however, an open question how close the analogy is. The structural resemblance has very local character only, and in the Fe sublattice in Fe_4N, the Fe-Fe separation is about 8% higher than in bcc Fe. Moreover, the Fe sublattice in Fe_4N has fcc structure and the presence of a surface reconstruction in thin $Fe_4N(001)$ films has been observed[26] under specific conditions.

Adsorption of oxygen on iron does not suppress significantly[29] or even slightly enhance surface and subsurface magnetization.[11,30,31] In a simple model, it has been predicted[32] that C and N reduce the magnetic moments at surface and subsurface Fe(001) atoms. This trend has been confirmed by more realistic calculations.[10,12] Also magnetism in nitridized Fe films or nanoparticles has been studied.[33,34,36] The experiments show that the Curie temperature and other magnetic properties of the sample can be seriously modified by nitrogen adsorption or absorption.

The examples we have given show that attempts to gain new information on the nitrogen effect upon iron surfaces are most welcome. In this communication we present density-functional calculations of regular nitrogen structures at the Fe(001) and Fe(110) surfaces or below them.

II. MODEL AND COMPUTATIONAL DETAILS

To perform spin-polarized density-functional electronic-structure calculations, the DACAPO code[37–39] was used. It is a plane-vawe code using ultrasoft Vanderbilt pseudopotentials to analyze periodic structures.

The choice of systems and details of the calculation are similar as those employed in a recent study of oxygen on Fe.[11] We consider six-layer Fe(001) and Fe(110) bcc slabs in the supercell approach. At or below the slab "upper" surface, $p(1\times1)$, $p(2\times1)$, $c(2\times2)$, or $p(2\times2)$ nitrogen atomic patterns are arranged. The structures are well known and their detailed description is given, e.g., in Refs. 3 and 11. For the reader's convenience, we show the (2×2) and (2×1) surface geometries also in Figs. 1 and 2.

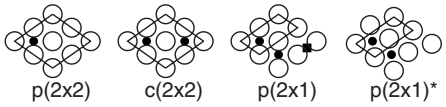

FIG. 1. Geometry of (2×2) and (2×1) superstructures above the Fe(110) surface (top view). Fe atoms are depicted as open circles and nitrogen as black dots in the long-bridge sites. Elementary cells are limited by lines. The tetragonal subsurface site below the short-bridge position is represented by a black square in the $p(2\times1)$ structure. The $p(2\times1)^*$ structure represents the relaxed geometry described in the text and in Table III.

The choice of high-symmetry adsorption sites is confirmed by low-energy electron diffraction (LEED) for the Fe(001) surface;[3,7] in other cases, it conforms to generally observed trends (see especially the related studies in Refs. 11 and 12). For subsurface nitrogen, however, also broken-symmetry geometries appear. The upper three Fe layers and nitrogen atoms are allowed to relax. Whereas for some patterns [mainly (1×1) ones] only vertical movements are possible because of the geometry constraints, for other overlayers also deformations parallel to the surface are allowed and appear to be important. The slabs within the supercell are separated by a vacuum layer about 14 Å wide. The gradient-corrected Perdew-Wang form of density functional[35] (PW91) is used, and the energy cutoff for plane waves is 400 eV. For the two-dimensional Brillouin zone, the Monkhorst-Pack (8×8) mesh is used for (1×1) structures with corresponding change for superstructures. The dipole correction compensating the work-function jump between the two nonequivalent slab surfaces is switched on. The geometry optimization is done by using the conjugate gradient algorithm. The magnetic moments on the slab surfaces remain practically unaffected when nitrogen is adsorbed on the opposite face, which confirms that the slab is thick enough to describe correctly the magnetization.

The N_2 molecule ground state is known to be nonmagnetic ($^1\Sigma_g^+$) with the N-N distance of 1.10 Å; our calculations provide the value 1.12 Å. For ferromagnetic bcc iron we find a lattice constant $a=2.855$ Å and accept it when constructing iron slabs (experimental value is 2.87 Å). The theoretical magnetic bulk momentum $2.29\mu_B$ per Fe atom is slightly

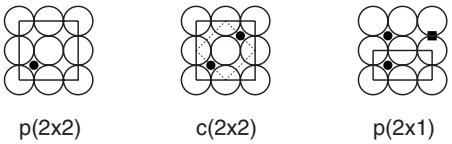

FIG. 2. Geometry of (2×2) and (2×1) superstructures above the Fe(001) surface (top view). Fe atoms are depicted as open circles and nitrogen as black dots in the fourfold (hollow) sites. Elementary cells are limited by lines; for $c(2\times2)$ both choices (2×2) and $(\sqrt{2}\times\sqrt{2})R45°$ (dotted lines) are shown. The tetragonal subsurface site below the bridge position is represented by a black square in the $p(2\times1)$ structure.

higher than the experimental value $2.22\mu_B$. These results are consistent with other theoretical values: Sorescu[12] reports several calculations (see also Ref. 11) for bulk iron. The calculated lattice constants and magnetic moments, respectively, fall into the range 2.831–2.865 Å and $2.20\mu_B$–$2.32\mu_B$. To assess local magnetic moments, we use atomic sphere with the bulk Wigner-Seitz radius r_{WS} = 1.41 Å for Fe and the covalent radius r_N=0.7 Å for nitrogen. We shall pay attention mainly to magnetic moments on Fe atoms placed close to N. With increasing Fe-N separation, the iron moments converge quickly with some oscillations, to ideal-slab values.

As usual, the adsorption (or absorption) energy is evaluated as

$$E_{ad} = [E(\mathrm{N} + \mathrm{Fe\ slab}) - E(\mathrm{Fe\ slab}) - 0.5nE(\mathrm{N}_2)]/n, \quad (2)$$

where n is the number of nitrogen atoms in the elementary cell and $E(\cdots)$ are the computed total energies of particular systems. Since only energy differences are of interest, one can subtract the nitrogen DFT atomic energies from the total energies. Then, clearly, $0.5E(\mathrm{N}_2) = -0.5D(\mathrm{N}_2)$, where D is the molecule dissociation energy. We get thus into the range of "meaningful" chemical-potential values for N as we shall see soon. One should remember that particular dissociation energies differ when comparing the present values with literature findings for related C or O adsorption-absorption systems. The experimental energies for the C_2, N_2, and O_2 molecules read 6.2, 9.8, and 5.1 eV, respectively. At zero temperature, the adsorption is energetically favorable if

$$E_{ad} < 0. \quad (3)$$

For nonzero temperature, this inequality modifies to

$$\mu_N(\mathrm{solid}) - \mu_N(\mathrm{N}_2\ \mathrm{gas}) < 0, \quad (4)$$

where the chemical potentials of nitrogen in the solid and N_2 gas phases, respectively, appear. For *ordered* solid structures, μ_N(solid) does not depend significantly on pressure and temperature, and can be approximated by the first difference in Eq. (2). For low pressure or high temperature, the second term in Eq. (4) can be essentially lower (larger in absolute value) than $-0.5D$. In this case, the ordered solid phase is thermodynamically less stable than predicted by Eq. (3). Since one has to minimalize the Gibbs free energy per unit surface area and not per nitrogen atom, the destabilization will be more marked for high-coverage phases.[11]

Let us now turn to compound formation. Its growth can start if the difference in Eq. (4) is zero (equilibrium condition). The change of standard chemical potentials,[40] ΔH^0 and ΔG^0, per N for Fe_4N (and probably for other Fe-rich nitrides[21]) formation is small[13] (~0.1 eV), and the expression in Eq. (2) is consequently also close to zero. Hence, $\mu_N(\mathrm{N}_2\ \mathrm{gas}) \sim -0.5D(\mathrm{N}_2)$ at gas-nitride equilibrium. Hence, we can use approximately the calculated zero-temperature energies near this equilibrium. For oxygen, the situation is quite different since the change of standard chemical potentials for the formation of stable oxides is larger by an order of magnitude and the process is exothermic.[13] This means that at oxide-free surfaces always $\mu_O(\mathrm{O}_2\ \mathrm{gas}) < -0.5D(\mathrm{O}_2)$ and high-coverage surface structures are generally more or less destabilized.[11]

TABLE I. Calculated adsorption energy E_{ad} per nitrogen atom and work function Φ for nitrogen atoms at long-bridge sites above Fe(110) and fourfold sites above the Fe(001) surface, respectively. The work function is 4.86 eV [4.06 eV] for the clean relaxed Fe(110) [Fe(001)] surface. Negative E_{ad} stands for exothermic dissociative adsorption.

Surface	Coverage (ML)	Structure	E_{ad} (eV)	Φ (eV)
(110)	0.25	$p(2\times2)$	−1.28	5.07
	0.50	$c(2\times2)$	−0.67	5.27
	0.50	$p(2\times1)$	−0.54	5.30
	1.00	$p(1\times1)$	0.82	6.44
(001)	0.25	$p(2\times2)$	−1.58	4.29
	0.50	$c(2\times2)$	−1.59	4.35
	0.50	$p(2\times1)$	−1.27	4.40
	1.00	$p(1\times1)$	−0.90	4.43

III. RESULTS AND DISCUSSION

A. Surface nitrogen

Properties of the nitridized Fe(110) and Fe(001) surfaces are similar in several respects. It is thus convenient to start with some comments of general character. With the exception of $p(1\times1)$N/Fe(110), the dissociative adsorption is exothermic (Table I). The adsorption is energetically more favorable on the Fe(001) surface. This is an obvious result since the coordination of Fe atoms on the open (001) surface is lower. The adsorption energies are smaller than for oxygen.[11] When comparing the values, however, one should take into account that the dissociation energy of N_2 is essentially higher than that of O_2. We have also checked the "non-self-consistent" (i.e., when the input geometries and electronic densities are calculated with the PW91 density functional) energies yielded by the revised Perdew-Burke-Ernzerhof (RPBE) form of DFT.[2,38] The RPBE adsorption energy is always lower by about 0.4 eV per nitrogen atom. Just the same value (0.79 eV per molecule) was obtained by Jenkins (2.80 versus 2.01 eV; see the last paragraph on p. 1433 of Ref. 10) for N on Fe(211). The weak dependence of this difference on geometry is remarkable since one would expect a stronger variation with the nitrogen coordination (the RPBE form is devised to reduce the tendency of DFT to favor highly coordinated sites). The calculations show that the work function grows with the concentration of N (Table I). This is in agreement with experiments whereas the reverse trend is observed[5,3] for nondissociative N_2 adsorption. The rise of the work function is consistent with the orientation of the dipole layer originating from the concentration of electronic charge near N.[10] The effect of oxygen on the work function is similar.[11]

Nitrogen produces considerable deformations mainly in the two upmost Fe layers (Tables II and III). It is important

TABLE II. Relaxations Δ_{ij} of the vertical interlayer distance for the (110) and (001) clean and N-covered iron surfaces. The relaxations are calculated with respect to ideal bcc iron slabs. z is the height of adsorbed N above the Fe surface [each layer level is defined by the iron nearest neighbor (NN) of nitrogen in that layer]. d is the nitrogen distance to its iron neighbors: for the (110) face we give the separation from first and second NN, for the (001) one, separation from first NN in the surface and subsurface Fe layer, respectively.

Surface	Coverage (ML)	Structure	Δ_{12} (%)	Δ_{23} (%)	Δ_{34} (%)	z (Å)	d (Å)
(110)	0.00	$p(1\times1)$	−0.23	0.26	−0.09		
	0.25	$p(2\times2)$	0.01	0.40	0.00	0.70	1.80; 1.98
	0.50	$c(2\times2)$	−0.13	−4.27	1.39	1.01	1.75; 2.13
	0.50	$p(2\times1)$	2.25	2.39	0.61	0.60	1.83; 1.89
	1.00	$p(1\times1)$	7.07	1.26	1.52	0.98	1.73; 2.24
(001)	0.00	$p(1\times1)$	−2.26	1.66	0.04		
	0.25	$p(2\times2)$	10.23	−7.73	1.93	0.39	1.98; 1.96
	0.50	$c(2\times2)$	11.88	−4.60	2.69	0.30	2.04; 1.90
	0.50	$p(2\times1)$	12.50	−7.39	2.21	0.31	1.97; 1.92
	1.00	$p(1\times1)$	17.01	−3.29	1.16	0.18	2.03; 1.85

to remark that, for lower nitrogen coverage, more degrees of freedom appear in the form of possible in-plane deformation and buckling (nonzero vertical separation between nonequivalent atoms in a layer) of the Fe layers.

As Table IV shows, the magnetic moments of iron atoms close to N are markedly reduced. Apparently, the number of nitrogen neighbors and the Fe-N separation are the most important parameters. For analogous oxygen structures, on the other hand, an enhancement of iron magnetism is reported.[11] It has been suggested that the Fe-O interaction has some features in common with that in iron oxides[11] and that the expansion at the surface probably also contributes. Let us note that for oxygen on the open Fe(211) surface, some magnetization lowering has been predicted.[10] For nitrogen, the N($2p$) states lie closer to E_F because of the lower number of electrons, which can make their interaction with Fe($3d$) states more intense. Nitrogen gains always a small magnetic moment antiparallel to the iron moment. This seems to be a general trend for N or C (but not for O) chemisorbed on Fe or Co surfaces[10,12,41,42] (cf. also Ref. 19 for nitrides). Also for chemisorption of Li, B, P, or Ca on Ni(210), antiferromagnetic coupling between adatom and Ni was predicted.[43] An attempt to rationalize such a moment orientation has been undertaken in Ref. 44.

TABLE III. Cartesian coordinates x,y,z of the nitrogen atom (N) and of nonequivalent iron atoms at surfaces ($1a$,$1b$) and subsurfaces ($2a$,$2b$) in the (2×1)N/Fe(110) structure. The Fe atom positions in the ideal bcc lattice are given in parentheses. The z axis is oriented along the slab normal. The (2×1) 2-dim cell is defined by vector $\mathbf{e}_1=(4.038,2.855)=2(2.019,1.428)$ and $\mathbf{e}_2=(2.019,-1.428)$. All values are in Å. For the third slab layer, the Fe atoms reside very close to ideal lattice sites.

Atom	x	y	z
N	0.000	0.000	0.704
$1a$	1.767 (2.019)	0.283 (0.000)	0.106 (0.000)
$1b$	0.251 (0.000)	−1.710 (−1.428)	0.106 (0.000)
$2a$	0.000 (0.000)	0.000 (0.000)	−1.958 (−2.019)
$2b$	2.019 (2.019)	1.428 (1.428)	−2.013 (−2.019)

1. Adsorption on the Fe(110) surface

Experiments show[6] that at Fe(110), nitrogen forms first a (2×3) pattern. Additional information on its geometry is not available. At higher coverage, a complicated reconstructed structure, the nature of which is not known, is revealed by LEED.[6] These authors speculate about a possible similarity with the $Fe_4N(111)$ surface. We believe that it is enlightening to analyze the sequence of regular structures even under these circumstances. Hopefully, at least the low-concentration models are realistic since the local Fe-N interactions should prevail over the N-N ones. Besides that, we can get an approximate idea about the dependence of various properties of the system upon nitrogen concentration.

We choose the high-symmetry long-bridge (hollow) site as the adsorption site (see Fig. 1 and Ref. 11). We have ruled out the unlikely possibility that it represents a saddle point rather than an energy minimum by evaluating forces acting on a slightly displaced nitrogen atom at coverage $\theta=0.25$. Table I reveals that the adsorption energy is quickly decreasing with nitrogen concentration, the process becoming endothermic at full coverage. The energy gain per unit surface is almost the same for the primitive and centered (2×2) structures and is larger than for the $p(2\times1)$ pattern. Hence, the low-coverage phase will become most stable at not very high pressures due to the low value of the nitrogen chemical potential in the gas atmosphere (see Sec. II). The presence of surface reconstructions (supposing that they are not very large ones) can modify slightly this conclusion.

The work function increases with coverage and presents a big jump at $\theta=1$. An analogous behavior has been reported for oxygen deposition.[11] The character of deformations due to N differs from structure to structure (Table II). Particularly, in $p(2\times1)$ and $p(2\times2)$ nitrogen phases, the system has enough freedom to shorten significantly the distance of N

TABLE IV. Magnetic moments (in μ_B) calculated for nitrogen and the first three iron layers. For layers with nonequivalent Fe atoms, values for atoms closest to nitrogen are given.

Surface	Layer	Clean	$p(2\times2)$	$c(2\times2)$	$p(2\times1)$	$p(1\times1)$
(110)	N		−0.10	−0.08	−0.03	−0.03
	1	2.69	1.89	0.81	1.77	0.42
	2	2.38	2.53	2.48	2.62	2.55
	3	2.33	2.32	2.41	2.36	2.40
(001)	N		−0.08	−0.06	−0.06	−0.04
	1	3.05	2.79	2.71	2.53	2.55
	2	2.38	1.95	1.84	1.91	1.84
	3	2.35	2.44	2.42	2.44	2.38

to its second-nearest iron neighbors. For the $c(2\times2)$ overlayer, the in-plane deformations are less effective and there is buckling of about 0.3 Å at the Fe surface. Quite remarkable is the geometry of the $p(2\times1)$N (θ=0.5) structure. In Table III the relaxed geometry is displayed in detail; it can be easily verified that an inhomogeneous surface lattice is formed in which four-tuples of surface Fe atoms surrounding N change their arrangement from rhombus almost to square (Fig. 1). This large relaxation is enabled by the low symmetry of the (2×1) phase: the only nontrivial symmetry operation reads $(x,y,z)\rightarrow(-x,-y,z)$ with the z axis along the surface normal. Hence, an effort to shorten some bonds and enlarge thus the coordination of N chemisorbed on Fe(110) is apparent. This effort might be the mechanism behind the reconstruction observed in the Ref. 6 since, at higher θ, it cannot be fullfilled without considerable geometry changes.

The effect of nitrogen upon magnetization follows the picture drawn before. The magnetic moments on surface Fe atoms close to N are significantly reduced (Table IV). The huge effect observed for $c(2\times2)$N and $p(1\times1)$N clearly correlates with the considerable Fe-N bond shortening (Table II); the nitrogen concentration is another factor of importance. On subsurface Fe atoms well separated from nitrogen, a moderate magnetization enhancement takes place, probably due to the weakened interaction with the surface Fe atoms. On nitrogen, a small magnetic moment appears with antiparallel orientation. The overall situation is completely different from that for oxygen on Fe(110),[11] where a moderate increase of magnetization on the surface Fe atoms and ferromagnetic Fe-O coupling occur.

2. Adsorption on the Fe(001) surface

At the (001) surface, the most likely [in the light of numerous experimental and theoretical results on atomic adsorption at transition-metal (001) surfaces] adsorption site is the symmetric and highly coordinated hollow (fourfold) site. For the $p(2\times2)$ overlayer we have verified the stability by calculating forces acting on slightly displaced N. Actually, stability of this site is confirmed by LEED studies[3,7] that find the $c(2\times2)$ order. Measurements, that have been performed in the ultrahigh vacuum regime do not find the $p(1\times1)$ phase on Fe(001). A tentative explanation might be that the experiments were performed at low pressure where the large negative value of the chemical potential for N in the gas phase hinders its formation. Let us mention that for oxygen on Fe(001), both disordered and ordered $p(1\times1)$ phases can be prepared,[45] whereas for carbon an interesting superstructure at coverage 2/3 has been prepared by segregation from the bulk.[46]

The dissociative adsorption of N is now exothermic (Table I) for all structures studied. It is interesting to mention a rather weak dependence of adsorption energy on coverage for Fe(001)—an effect present also for adsorbed O (Ref. 11) and C (Ref. 12). We think that the reason is that each nitrogen atom bonds to "its own" subsurface iron atom, whereas the bonding capacity of iron atoms at Fe(110) surface becomes saturated at higher nitrogen coverage. The work function rises after adsorption but its coverage dependence is rather weak.

The nearest neighbor of the nitrogen adatom is the subsurface iron atom, with the separation (Table II) resembling the N-Fe distance 1.9 Å in Fe_4N. The nitrogen separation from surface iron atoms is larger. Similar values are obtained for carbon deposition.[12] The data of Table II point out the tendency to shorten distances between N and its four surface iron neighbors, which is successful for the low-coverage structure $p(2\times2)$ and low-symmetry pattern $p(2\times1)$.

Magnetic moments are more reduced on subsurface iron atoms than on surface ones for the two (2×2) structures, whereas for the remaining two structures the effect is almost the same (Table IV). For subsurface-atom moments, the Fe-N separation is the main parameter; for Fe surface atoms also the increase of its nitrogen neighbors tends to diminish the magnetization. On nitrogen, we again find small magnetic moments that couple antiferromagnetically to iron.

Electronic properties ($2p$-electron level occupation, electronegativity) vary by the same or similar value in the sequence C-N-O. Hence, one might expect a monotonous and regular adsorbate-induced change of the surface and subsurface iron magnetization in the C-N-O sequence. Comparison of magnetic moments in Ref. 12 with the present ones (Table V) as well as the data from the Table 10 of Ref. 10 indicate, however, that the effect of C and N upon iron magnetism is comparable and different from the oxygen case. The moderate adsorbate moments vary, however, clearly monotonously in the above sequence according to Table 10 of Ref. 10.

The results of the calculation can be compared with experimental data for $c(2\times2)$N/Fe(001). The change of the

TABLE V. Average magnetic moments (in μ_B) in the first three iron layers calculated for nitrogen- or carbon-containing Fe(001) slabs. The moments are presented in the form m_N/m_C for the N and C cases, respectively. $p(2\times2)$, $c(2\times2)$, and $p(1\times1)$ are surface overlayers; $p(2\times2)o$ and $p(1\times1)o$ stand for N or C absorbed in octahedral subsurface sites. The results for carbon-containing slabs are from Table V of Ref. 12.

Layer	$p(2\times2)$	$c(2\times2)$	$p(1\times1)$	$p(2\times2)o$	$p(1\times1)o$
1	2.79/2.72	2.71/2.49	2.55/2.21	2.98/2.88	2.88/2.53
2	2.35/2.38	2.23/2.15	1.84/1.88	2.26/2.24	2.04/2.05
3	2.44/2.48	2.42/2.47	2.38/2.49	2.39/2.45	2.06/2.20

work function by 0.29 eV is in good accordance with measurement.[3] Also the N-Fe(surface) separation is in excellent agreement with experiment[7] whereas the distance N-Fe(subsurface)=1.9 Å is somewhat longer than the experimental value 1.83 Å. It remains to check whether inclusion of the calculated buckling of ~0.1 Å in the subsurface layer (no such effect was included in the LEED data evaluation) might modify the situation. It is worthy to note that a similar geometric structure has been predicted in a recent DFT study[47] for nitrogen on Cu(001). The nitrogen-derived photoemission features about 5 eV below the Fermi level[3] also correlate with our local density of states (LDOS) (Fig. 3). The marked dip in minority-spin LDOS at E_F evaluated for the subsurface Fe atom confirms once more the strong interaction of this atom with N. Another remarkable point is that the spin asymmetry A at E_F $[A=(\rho_\uparrow-\rho_\downarrow)/(\rho_\uparrow+\rho_\downarrow)$, where $\rho_\uparrow$, $\rho_\downarrow$ stand for iron majority- or minority-spin LDOS at $E_F]$ differs, in both magnitude and sign, for surface and subsurface iron atoms, respectively. For d-electron states, $A=-0.65$ at surface and $A=0.38$ at subsurface Fe atoms below N. It would be interesting to analyze to what extent a similar situation at surfaces or interfaces might affect the predictions of transport properties based on bulk calculations[28] (see the Introduction) when current transversal to the surface is considered. The reason is that, as a rule, there is some correlation[28] between spin-polarized conductivity and the most outstanding LDOS features at E_F.

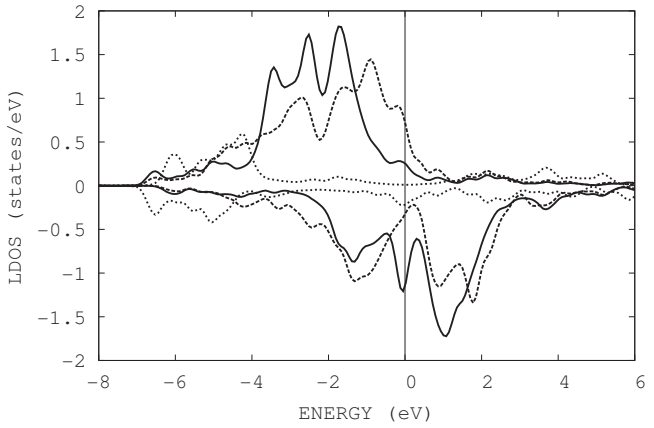

FIG. 3. Spin-resolved local densities of electronic states (LDOS) for the $c(2\times2)$N/Fe(001) system. Spin ↑ states are displayed in the upper half of the figure, spin ↓ (negative LDOS) states in the lower part of the figure. Note that spin ↑ states are the majority-spin states for Fe and minority-spin states for N. Solid and dashed lines correspond to the d-electron LDOS at surface or subsurface iron atoms, respectively. The dotted lines mark s,p-electron nitrogen states. The Fermi level coincides with the energy zero.

B. Subsurface nitrogen

Results for subsurface nitrogen deposition are more complex than for adsorption. In Ref. 11 some regular structures turned out to be unstable. We find yet additional unstable structures especially for the (110) surface. The dissociative absorption is always endothermic (Table VI) but for some structures below the (001) surface the energy loss is not large. This conforms to the experimental findings for bcc iron we mentioned in the Introduction. The crystal lattice around N is considerably deformed as shown by the values of interplanar expansion in Table VII. Nevertheless, none of these structures can be thermodynamically stable. Indeed, μ_N (N_2 gas) can vary from large negative values to roughly $-0.5D$ (N_2) when the three-dimensional nitride growth starts (Sec. II). In this range, however, the endothermic subsurface phases cannot have lower Gibbs free energy per unit area than, e.g., the highly energetically favorable $p(2\times2)$N overlayers. (Let us remind the reader that destabilization by lowering the chemical potential of N in the N_2 gas is least marked for low-concentration structures—i.e., $\theta=0.25$ in our case.) The energy differences between the surface and sub-

TABLE VI. Calculated absorption energy per N subsurface atom, E_{ab}, and work function Φ. For the subsurface nitrogen structure $[p(2\times2)$ or $p(1\times1)]$ the absorption site is specified by o (octahedral) or t (tetrahedral). "+" points to the presence of a $p(1\times1)$N surface overlayer. To evaluate E_{ab} in the latter case, the N_2 molecule plus the Fe slab with a $p(1\times1)$N overlayer is considered as reactant entering the dissociation.

Surface	Structure	E_{ab} (eV)	Φ (eV)
(110)	$p(2\times2)o$	0.65	4.93
	$p(1\times1)o$	1.42	4.45
	$p(1\times1)t$	0.87	5.02
(001)	$p(2\times2)o$	0.20	4.10
	$p(2\times2)o+$	0.73	4.39
	$p(1\times1)o$	0.28	4.45
	$p(1\times1)o+$	0.52	4.41
	$p(1\times1)t$	0.47	4.55
	$p(1\times1)t+$	2.05	6.18

TABLE VII. Relaxations Δ_{ij} of the vertical interlayer distances for the two clean and N-covered iron surfaces with subsurface nitrogen present. The notation for various structures is the same as in Table V. The relaxations are calculated with respect to ideal bcc slabs. z_1 (z_2) is the height of adsorbed N above the surface (height of the subsurface N above the subsurface layer). Each layer level is defined by the iron nearest neighbor (NN) of subsurface nitrogen in that layer. d_1 (d_2) is the surface (subsurface) nitrogen distance to its iron NN in surface and subsurface layer [two values for Fe(110) with $p(2\times2)$N in subsurface octahedral positions], respectively. For subsurface nitrogen in octahedral subsurface sites below Fe(001) and in the $p(2\times2)$ geometry below Fe(110), we give also its separation from its NN in the third Fe layer.

Surface	Structure	Δ_{12} (%)	Δ_{23} (%)	Δ_{34} (%)	z_1 (Å)	z_2 (Å)	d_1 (Å)	d_2 (Å)
(110)	$p(2\times2)o$	−3.68	4.89	2.22		−0.20		2.14, 1.74, 1.93, 1.92
	$p(1\times1)o$	46.54	2.68	−0.50		1.23		1.73, 1.88
	$p(1\times1)t$	37.65	0.30	0.99		1.40		1.85, 1.87
(001)	$p(2\times2)o$	32.36	19.82	−9.35		0.12		1.84, 2.01, 1.83
	$p(2\times2)o+$	37.90	23.74	−12.59	−0.05	0.02	1.99,1.92	1.95, 1.97; 1.79
	$p(1\times1)o$	32.75	25.39	−1.91		0.03		1.87, 2.02, 1.85
	$p(1\times1)o+$	39.52	30.22	−2.76	0.08	−0.03	2.02,2.07	2.02, 2.02; 1.82
	$p(1\times1)t$	65.16	6.37	−0.45		1.24		1.82, 1.89
	$p(1\times1)t+$	85.33	6.87	0.49	0.59	1.16	2.10,3.23	2.06, 1.84

surface structures are large, and moderate reconstructions can hardly change the conclusion. Still, a brief analysis of these structures might be of methodical interest since it manifests the interplay between the energy, local geometry, and magnetism. Naturally, the presence of some subsurface-disordered nitrogen at low concentration stabilized by entropy is expected similarly as in the bulk case. The $p(2\times2)$ models can give some crude idea about the properties of these absorbed atoms. The non-self-consistently evaluated RPBE energies (see Sec. III A) yield further destabilization, again roughly by 0.4 eV per nitrogen atom as in the case of adsorption. Similarly as for the surface adsorption, the absorption energies reflect also the large energy necessary to dissociate the N_2 molecule.

Magnetic moments follow a similar trend as we have seen for surface overlayers, but in a few exceptional cases nitrogen couples ferromagnetically to iron (Table VIII). Because of large local deformations introduced by nitrogen, the change of the Fe-Fe separation can also seriously influence the magnetization.

In the following we denote by o and t the octahedral and tetrahedral subsurface sites, respectively, and by + the presence of the $p(1\times1)$N overlayer.

1. Absorption below the Fe(110) surface

The dissolution of nitrogen below the surface is endothermic for all cases considered (Table VI) and thermodynamically unstable as discussed above.

For the subsurface $p(1\times1)o$ order with N at the octahedral site (site below a surface Fe atom), the work function is lowered, whereas it increases for the other two structures. Since we know from experiments that the (110) surface is reconstructed at higher nitrogen coverage and that the ideal $p(1\times1)$N overlayer is energetically highly unfavorable (Table I), we do not calculate the dissolution of nitrogen below nitrogen-covered Fe(110) as has been done in Ref. 11 for oxygen. For the $p(2\times2)t$ structure, nitrogen segregates above the surface in the course of geometry optimization, when nitrogen atoms are placed originally into tetrahedral subsurface sites (Fig. 1). For the $p(2\times2)o$ geometry nitro-

TABLE VIII. Magnetic moments (in μ_B) calculated for iron atoms in the first three layers (m_1–m_3) and for surface (m_{N1}) or subsurface (m_{N2}) nitrogen. The notation for various structures is the same as in Table V.

Surface	Structure	m_1	m_2	m_3	m_{N1}	m_{N2}
(110)	$p(2\times2)o$	2.70	1.72, 2.25	2.13		−0.08
	$p(1\times1)o$	1.71	1.94	2.48		−0.16
	$p(1\times1)t$	1.68	1.44	2.43		−0.13
(001)	$p(2\times2)o$	2.78	2.15	1.76		−0.09
	$p(2\times2)o+$	2.78 (2.25[a])	1.89	1.65	0.00	−0.05
	$p(1\times1)o$	2.88	2.04	2.06		−0.02
	$p(1\times1)o+$	2.67	1.87	1.97	0.10	0.02
	$p(1\times1)t$	2.44	1.79	2.53		−0.07
	$p(1\times1)t+$	2.47	1.76	1.55	−0.19	−0.12

[a]Magnetic moment at another two Fe atoms in the elementary cell of the same layer.

gen moves actually *below* the subsurface layer (negative z_2 in Table VII). Nevertheless, we include this structure since it might represent a realistic case of general interest. Because of horizontal deformations, the vertical relaxations of the iron lattice are not large (Table VII). The buckling in the surface (subsurface) Fe sheet is about 0.2 Å (0.1 Å). The four Fe neighbors of N in the subsurface layer are considerably displaced to shorten the Fe-N separations (Table VII). They form almost a (not exactly planar) square, resembling thus partly a situation met previously in surface chemisorption. The whole geometry can, to some extent, remind one of a considerably deformed neighborhood of N in the Fe_4N crystal. For the small (1×1) cell, there is not freedom enough for deformations to enable escape of the subsurface nitrogen and, hence, the systems are stable. Room for nitrogen atoms is gained by a large vertical surface expansion (Table VII) because of the impossibility of planar deformations.

Nitrogen atoms are rather well separated from the iron surface in the $p(2\times2)o$ phase and magnetic moments on their first nearest Fe surface neighbor are large (free-surface-like; cf. Tables VIII and III). Magnetization of second- and third-layer Fe atoms is reduced in dependence on their distance from N (Tables VII and VIII); changes in the Fe-Fe distance have undoubtedly also some role. In the $p(1\times1)o$ and $p(1\times1)t$ phases similar reasons decide upon the magnetization drop in the first two layers. The third Fe layer being sufficiently separated from nitrogen atoms bears a bulklike magnetic moment.

2. Absorption below the Fe(001) surface

Deposition of nitrogen in octahedral or tetrahedral subsurface positions, both below the clean Fe(001) surface and below the surface covered by a $p(1\times1)$N overlayer with adatoms above hollow sites, are considered in analogy to Ref. 11. (In Ref. 12 the tetrahedral site is denoted as octahedral $S2$ configuration since, by including yet two Fe atoms from the third layer, one gets a deformed Fe octahedron.) When both surface and subsurface nitrogen are present, we evaluate, in analogy to Ref. 11, the nitrogen absorption energy E_{ab} by considering the N_2 molecule plus Fe slab with a $p(1\times1)$N overlayer as the reactants entering the dissociative absorption.

In full analogy to the results for oxygen[11] we find that in the $p(2\times2)t$ arrangement the nitrogen segregates at the surface (moves to the second subsurface layer) when the surface is free (covered by a N overlayer). To relieve the energetical barrier and allow the escape of N from the subsurface layer, two Fe atoms "give the way" by enlarging their separation considerably (cf. the geometry of the subsurface $S2$ site for carbon in Ref. 12). A similar rearrangement is not possible for the dense $p(1\times1)$N subsurface geometries. In Ref. 12 the tetrahedral site is not unstable but is energetically highly unfavorable for carbon absorption.

Contrary to oxygen and carbon cases,[11,12] nitrogen dissolution into stable configurations is always endothermic (Table VI). The octahedral sites are preferred over tetrahedral ones. The $p(2\times2)o$ structure can be considered again as a deformed germ of a $Fe_4N(001)$ film. We find a large work function value for the system $p(1\times1)t+$ (Table VI) as well as a small or moderate increase of the work function for the remaining subsurface structures correlated with calculations for the oxygen (Ref. 11, Table III).

There is a nitrogen-induced expansion in the surface region as is seen from values of Δ_{12} and Δ_{23} in Table VII; negative values of Δ_{34} are due to the fact that nitrogen pushes the third-layer Fe atoms placed just below it towards the fourth layer. The nitrogen atoms show some tendency to be placed in the iron-atom planes (small z_1, z_2 values). The latter statement is not completely rigorous for $p(2\times2)o$ structures because of considerable buckling in the surface layer [$\sim$0.6 Å (0.3 Å) in the absence (presence) of a nitrogen overlayer at the surface] and in the third layer ($\sim$0.2 Å). The small negative z_1 for the surface nitrogen in $p(2\times2)o+$ is caused by the fact that the reference-level Fe surface atom in Table VII is pushed up above the other Fe atoms, by subsurface N. The subsurface nitrogen layer moves actually below the second Fe layer for the $p(1\times1)o+$ complex (negative z_2 in Table VII) but it is possible to consider it rather as essentially residing in the subsurface iron plane because of the small z_2 value. Similarly, as for carbon [Ref. 12, Figs. 2(a) and 2(c)], we find a symmetry-broken state for N in octahedral subsurface sites: The surface iron atom just above N moves away from the symmetric site along the diagonal of the square surface lattice. The origin of the phenomenon can be understood as follows. The surface iron atom above the nitrogen is pushed upwards, weakening thus its interaction with other iron atoms. Since in the $p(2\times2)o$ phase the diagonal symmetry-breaking displacement brings the Fe atom closer to two of its surface Fe neighbors, two Fe-Fe bonds are shortened to 2.56 Å and get stabilized. There is also marked buckling (0.53 Å) in the surface layer, and nitrogen is slightly displaced along the diagonal in the opposite direction. For $p(1\times1)o$, the symmetry-breaking deformation is smaller and its effect on the energy, magnetic moments, and work function is negligible. Here, the stabilization consists probably in a minor improvement of bonding between surface and subsurface Fe layers, respectively.

The magnetic moments of iron atoms are again reduced by interaction with nitrogen. The effect is most sizable in the second and third iron layers at atoms close to N. For the $p(2\times2)o+$ complex, the surface-moment drop is not the largest one at the Fe atom that is closest to the subsurface nitrogen (Table VIII). This atom becomes simultaneously the surface atom most remote from the subsurface iron layer because of buckling, which works against the moment reduction. Hence, the Fe-Fe atomic separation is another factor that can control the magnetization. The magnetic moments of nitrogen atoms are small and are oriented antiparallel to iron moments in most cases. As seen from Table VIII, however, ferromagnetic coupling takes place for one, probably not realistic, structure $p(1\times1)o+$.

IV. CONCLUSIONS

We have presented extensive density-functional theory calculations for nitrogen adsorbed on Fe(110) and Fe(001)

surfaces, or absorbed below them. The results for adsorption on Fe(001) correlate well with the available measurements. For marked structural and work-function changes, the general trends often (but not always) agree with findings of recent theoretical studies performed for O or C atoms instead of N. Particularly, deposition of N just below the (110) surface seems to be energetically quite unfavorable. As far as magnetism is concerned, the present study resembles the case of carbon at Fe surfaces, but is quite different from the oxygen case. For lower nitrogen coverages, considerable lateral lattice deformations are found that cannot occur for dense $p(1\times1)$ nitrogen geometries. For the Fe(110) surface the chemisorption energy significantly decreases with nitrogen coverage θ for the simple structures considered here. For the $p(2\times1)$ superstructure (θ=0.5) we find marked geometry relaxations caused by N that indicate a tendency to form a structure in which the coordination of nitrogen is higher. This picture supports previous ideas suggested to explain the experimentally found reconstruction of Fe(110) induced by N.

The dissolution of N below the surface is always endothermic and some symmetric subsurface sites are unstable. Generally, considerable local deformations around the N site are met, and most structures are energetically highly unfavorable. We argue that all these structures are unstable also thermodynamically. Hence, we expect that the two-dimensional adlayers are succeeded by the growth of three-dimensional nitride(s) nuclei with low N concentration, as indicated by metallurgical studies.

In all cases, nitrogen reduces magnetization at neighboring iron atoms and, in almost all cases, acquires a small magnetic moment antiparallel to Fe magnetization. Such behavior seems common for N and C. The factor controlling iron magnetization is the Fe-N distance. Large changes of the Fe-Fe distance present especially close to the subsurface N are also important.

ACKNOWLEDGMENT

Š.P. is indebted to Université Louis Pasteur, Strasbourg, for kind hospitality and financial support.

*Corresponding author. Electronic address: stepan.pick@jh-inst.cas.cz

[1] B. I. Lundqvist, Vacuum **33**, 639 (1983).
[2] S. Dahl, A. Logadottir, C. J. H. Jacobsen, and J. K. Nørskov, Appl. Catal., A **222**, 19 (2001), and references therein.
[3] F. Bozso, G. Ertl, M. Grunze, and M. Weiss, J. Catal. **49**, 18 (1977).
[4] M. Alducin, R. Díez Muiño, H. F. Busnengo, and A. Salin, Phys. Rev. Lett. **97**, 056102 (2006); J. Chem. Phys. **125**, 144705 (2006).
[5] Z. Knor and V. Ponec, J. Catal. **10**, 73 (1968).
[6] F. Bozso, G. Ertl, and M. Weiss, J. Catal. **50**, 519 (1977).
[7] R. Imbihl, R. J. Behm, G. Ertl, and W. Moritz, Surf. Sci. **123**, 129 (1982).
[8] D. Haneman, Surf. Sci. **375**, 71 (1997).
[9] D. K. Escott, S. J. Pratt, and D. A. King, Surf. Sci. **562**, 226 (2004).
[10] S. J. Jenkins, Surf. Sci. **600**, 1431 (2006).
[11] P. Blonski, A. Kiejna, and J. Hafner, Surf. Sci. **590**, 88 (2005).
[12] D. C. Sorescu, Phys. Rev. B **73**, 155420 (2006).
[13] J. D. Fast, *Interaction of Metals and Gases* (Philips Technical Library, Eindhoven, 1965), Vol. 1, especially Sec. 7.8.
[14] A. A. Zhukhovitskii and L. A. Shvartzman, *Physical Chemistry* (Metallurgiya, Moscow, 1976) (in Russian).
[15] B. Appolaire and M. Gouné, Comput. Mater. Sci. **38**, 126 (2006).
[16] W. B. Pearson, *Handbook of Lattice Spacings and Structures of Metals* (Pergamon, Oxford, 1967).
[17] More often is used a very similar form of the van't Hoff equation for heat (enthalpy) of the reaction (Refs. 13 and 14). It leads to the same conclusion in our case.
[18] X. Luo and S. Liu, J. Magn. Magn. Mater. **308**, L1 (2007).
[19] A. Sakuma, J. Magn. Magn. Mater. **102**, 127 (1991).
[20] E. L. Peltzer y Blancá, J. Desimoni, and N. E. Christensen, Hyperfine Interact. **161**, 171 (2005).
[21] F. R. de Boer, R. Boom, W. C. M. Mattens, A. R. Miedema, and A. K. Niessen, *Cohesion in Metals: Transition Metal Alloys* (North-Holland, Amsterdam, 1988).
[22] A. N. Timoshevskii, V. A. Timoshevskii, and B. Z. Yanchitski, J. Phys.: Condens. Matter **13**, 1051 (2001).
[23] S. F. Matar, C. R. Chim. **5**, 539 (2002).
[24] S. F. Matar, J. Alloys Compd. **345**, 72 (2002).
[25] M. Ogura and H. Akai, Hyperfine Interact. **158**, 19 (2004).
[26] C. Navio, J. Alvarez, M. J. Capitan, D. Ecija, J. M. Gallego, F. Ynduráin, and R. Miranda, Phys. Rev. B **75**, 125422 (2007).
[27] A. Houari, S. F. Matar, M. A. Belkhir, and M. Nakhl, Phys. Rev. B **75**, 064420 (2007).
[28] S. Kokado, N. Fujima, K. Harigaya, H. Shimizu, and A. Sakuma, Phys. Rev. B **73**, 172410 (2006).
[29] M. Busch, M. Gruyters, and H. Winter, Surf. Sci. **600**, 4598 (2006), and references therein.
[30] H. Huang and J. Hermanson, Phys. Rev. B **32**, 6312 (1985).
[31] S. R. Chubb and W. E. Pickett, Phys. Rev. Lett. **58**, 1248 (1987).
[32] Š. Pick and H. Dreyssé, Surf. Sci. **394**, 192 (1997).
[33] C. M. Hsu, H. M. Lin, K. R. Tsai, and P. Y. Lee, J. Appl. Phys. **76**, 4793 (1994).
[34] W. B. Mi, F. He, Z. Q. Li, P. Wu, E. Y. Jiang, and H. L. Bai, J. Phys. D **39**, 911 (2006).
[35] J. P. Perdew, J. A. Chevary, S. H. Vosko, K. A. Jackson, M. R. Pederson, D. J. Singh, and C. Fiolhais, Phys. Rev. B **46**, 6671 (1992).
[36] W. L. Li, Y. Sun, and W. D. Fei, Appl. Surf. Sci. **252**, 4995 (2006).
[37] *Ab initio* pseudopotential code DACAPO developed at CAMPOS (Center for Atomic-Scale Materials Physics), Dept. of Physics, Techical University of Denmark, Lyngby; see www.camp.dtu.dk/campos
[38] B. Hammer, L. B. Hansen, and J. K. Nørskov, Phys. Rev. B **59**, 7413 (1999).

[39] S. Bahn and K. W. Jacobsen, CiSE **4**, 56 (2002).
[40] The superscript 0 means that the potentials are measured at temperature 298 K and pressure 1 atm. Because of the latter condition, the ideal-gas terms $RT \ln p$ are not included ($\ln 1 = 0$), and the potential change should be close to the internal energy change.
[41] Š. Pick and H. Dreyssé, Surf. Sci. **474**, 70 (2001).
[42] Š. Pick and H. Dreyssé, Surf. Sci. **540**, 389 (2003).
[43] W. T. Geng, A. J. Freeman, and R. Q. Wu, Phys. Rev. B **63**, 064427 (2001).
[44] Š. Pick and H. Dreyssé, Surf. Sci. **460**, 153 (2000).
[45] R. Moroni, F. Bisio, M. Canepa, and L. Mattera, Appl. Surf. Sci. **175-176**, 797 (2001).
[46] J. Fujii, G. Panaccione, I. Vobornik, G. Rossi, G. Trimarchi, and N. Binggeli, Surf. Sci. **600**, 3884 (2006).
[47] X.-M. Tao, M.-Q. Tan, X.-X. Zhao, W.-B. Chen, X. Chen, and X.-F. Shang, Surf. Sci. **600**, 3416 (2006).